

AD-A159 403

INTEGRATED OPTOELECTRONIC CIRCUITS UTILIZING INGAASP  
GROWN BY MOLECULAR BEAM EPITAXY(U) GEORGIA TECH  
RESEARCH INST ATLANTA E L MEEKS ET AL. 25 NOV 84

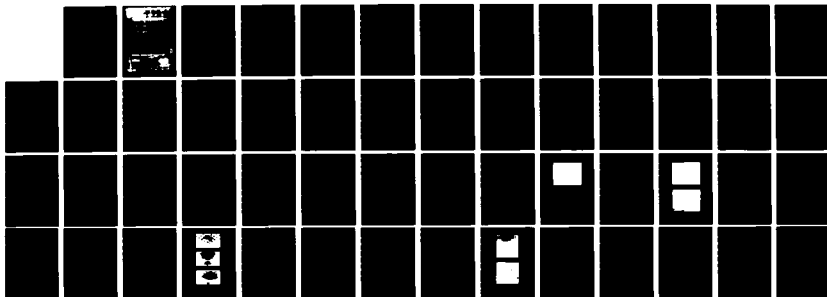
1/1

UNCLASSIFIED

N00014-83-K-2017

F/G 20/12

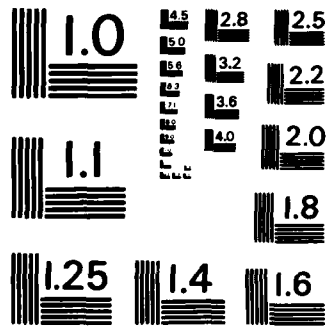
NL



END

FILMED

DTIC



MICROCOPY RESOLUTION TEST CHART  
NATIONAL BUREAU OF STANDARDS-1963-A

AD-A159 403

E. J.

Georgia Institute of Technology  
Atlanta, Georgia 30332

Report for period 1 January 1983 - 25 November 1984

Contract No. N00014-82-0-2017

Prepared for:

Naval Research Laboratory  
Washington, D. C. 20384

DTIC

SECRET

INTEGRATED OPTOELECTRONIC CIRCUITS UTILIZING  
InGaAsP GROWN BY MOLECULAR BEAM EPITAXY

Annual Report

E. L. Meeks, C. J. Summers and N. W. Cox

Georgia Tech Research Institute  
Georgia Institute of Technology  
Atlanta, Georgia 30332

Report for period 1 January 1983 - 25 November 1984

Contract No. N00014-8333-K-2017

Prepared for:

Naval Research Laboratory  
Washington, D. C, 20364

DTIC  
SELECTED  
SEP 23 1984  
S

A

## PREFACE

This report describes work primarily performed at the Georgia Institute of Technology, Georgia Tech Research Institute under Contract No. N00014-83-K-2017 during the period April 1st 1984 through 31 March 1985. Funding for the program is provided by the Naval Electronics Systems Command. The Scientific Officers responsible for the technical administration of the program are Dr. John E. Davey and Dr. Harry Dietrich of the Naval Research Laboratory.

TABLE OF CONTENTS

	Page
List of Tables .....	ii
List of Illustrations .....	iii
1.0 Background and Introduction .....	1
2.0 Experimental .....	5
2.1 Phosphorus in the Vacuum System .....	5
2.2 Source and Flux Monitoring .....	10
3.0 Material Growth and Characterization.....	17
3.1 InP Layers - "T Cell" .....	17
3.2 InP Layers - 125 gram source .....	25
3.3 Surface Features.....	28
3.4 Quaternary Layer Growth .....	30
4.0 CONCLUSIONS .....	45
5.0 REFERENCES .....	47

*Attch 12 files*

Mr.  
Mr.  
Avon  
Dist  
*A 1*



List of Tables

Table No.	Page
1. Quaternary Layers with Growth Conditions and Composition Results.....	34

## LIST OF ILLUSTRATIONS

Figure No.		Page
1.	Early Configuration of MBE System .....	7
2.	Final System configuration .....	8
3.	Phosphorus ( $P_2$ ) source with ion gauge flux monitor .....	11
4.	New large arsenic and phosphorus sources with cracker and flux monitor.....	13
5.	Phosphorus source temperature dependence on Phosphorus Pressure on $^{\circ}C$ .....	15
6.	Dependence of electron concentration on temperature .....	18
7.	Dependence of electron concentration on temperature for InP sample F1130.....	19
8.	Photoluminescence spectrum of InP sample F1110 at 77K.....	22
9.	Photoluminescence spectrum of InP sample F1118 at 77K.....	23
10.	Photoluminescence spectrum of InP sample F1130 at 77K.....	24
11.	Photoluminescence for films grown at 430 and 480C.....	27

12.	Photomicrograph of InP MBE surface and profile of a typical surface feature.....	29
13.	Phase contrast micrographs of layer surfaces grown at 430C and 480C. (500X).....	31
14.	Mobility of InP samples grown with $T_S = 430$ and $480C$ .....	32
15.	Electron concentration of InP samples grown with $T_S = 430$ and $480C$ .....	33
16.	Lattice Match data for $In_{1-x}Ga_xAs_yP_{1-y}$ Layers .....	35
17.	Reflection High Energy Electron Diffraction Patterns.....	37
18.	X-ray diffraction peaks for InP substrate.....	38
19.	InP substrate with quaternary layer G0524 .....	39
20.	Superposition of substrate curve and substrate plus quaternary layer G0628 with difference shown.....	40
21.	InP substrate with quaternary layer G0628.....	41
22.	SEM micrographs of quaternary surfaces. (2000X)....	42

## 1.0 BACKGROUND AND INTRODUCTION

The first work on molecular beam epitaxy (MBE) of InP was done 11 years ago by Farrow<sup>1,2</sup>. Since then, several authors<sup>3-11</sup> have reported successful growth of InP, but there is little agreement on the proper growth procedure. First, there are four different phosphorus sources in use: elemental red phosphorus which gives a flux of P<sub>4</sub> molecules,<sup>3,9,11</sup> a red phosphorus source in which the P<sub>4</sub> molecules are cracked to P<sub>2</sub> by passing them through a high (~900C) temperature nozzle,<sup>6,10,11</sup> InP bulk material which gives primarily P<sub>2</sub> molecules,<sup>1,5,7,11</sup> and phosphine which is cracked in a high temperature nozzle to give P<sub>2</sub> and H<sub>2</sub><sup>8,11</sup>. Also, epitaxial films have been grown over a wide substrate temperature range from 80C<sup>5</sup> to 650C<sup>10</sup> with variations in reported optimum growth temperature from 320C<sup>7</sup> to 580C<sup>10</sup>. Two authors<sup>5,7</sup> report inability to grow films at substrate temperatures above 410C because of the formation of In droplets on the surface which causes growth of InP whiskers.

There are also two different procedures used for substrate preparation. Some authors<sup>1,3,5,7,9</sup> report that an argon ion sputter and anneal of the substrate in the vacuum system is necessary prior to layer growth. Others<sup>6,8,10,11</sup> use only a heat treatment above 500C in a phosphorus flux very similar to the procedure used to grow GaAs layers.

At Georgia Tech we have tried all four of the phosphorus sources listed above plus two others (cracking phosphine and red phosphorus vapor in an arc discharge) and found none of them

without faults. The phosphorus flux from an InP source gradually decreases as the source is used, and the In flux gradually increases as the temperature is increased to compensate for the depletion of phosphorus. These changes are difficult to accommodate in the growth of InP layers because there is a minimum phosphorus to indium flux ratio that must be maintained for good epitaxy. The changing In flux also changes the growth rate and thus the impurity incorporation. For the growth of quaternary layers, a source that is not stable is even more difficult to use and good layers are reproduced only with careful manipulation of the sources as they age during growth. InP sources must be dimensionally small and open; otherwise, the  $P_2$  molecules polymerize to  $P_4$  and the major reason for using InP is lost. Small sources are depleted after only 3-4 hrs of growth time and must be replaced.

When red phosphorus is evaporated, it deposits as white phosphorus which has a high vapor pressure, is poisonous, and ignites spontaneously when exposed to air. The sticking coefficient of the  $P_4$  molecule is also much less than that of  $P_2$  on the hot InP substrates. Phosphorus to indium flux ratios  $> 100$  must be used to obtain good layers when  $P_4$  is the phosphorus source<sup>9</sup>. We have been able to grow good layers with flux ratios  $< 10$  using a  $P_2$  source but consume 2-3 grams of phosphorus per hour for a growth rate of one micron per hour. The flux ratio of  $> 100$  necessary for  $P_4$  would require a phosphorus consumption of 20-30 grams per hour for an equivalent growth rate. The distribution of

this much phosphorus into the MBE system can only be tolerated if special modifications are made. Tsang<sup>10</sup> introduced moving cryopanel into the MBE system in order to cope with the phosphorus needed to grow double heterostructure lasers by MBE.

The red phosphorus source can be improved by passing the phosphorus vapor through a high temperature nozzle to crack the  $P_4$  to  $P_2$ . This improves the sticking coefficient and reduces the phosphorus consumption by an order of magnitude. Also, the  $P_2$  molecules deposit in the system as red phosphorus which has a lower vapor pressure than the white form and does not ignite spontaneously when exposed to air. The cracked phosphorus source is an improvement but is far from ideal. This type source is presently being used at Georgia Tech to grow InP layers and consumes 2-3 grams of phosphorus per hour of growth for a growth rate of one micron per hour. On the present system, the cryopump must be regenerated and cleaned after about 40 grams of phosphorus is deposited in the MBE system.

Phosphine has been used successfully to grow MBE InP layers<sup>8,11</sup>. The phosphine is leaked into the vacuum system and cracked in a hot nozzle to give a flux of  $P_2$  and  $H_2$ . It has the advantage of being an "infinite" source since a large tank of phosphine can be kept outside the vacuum system. Its disadvantages are the same large phosphorus consumption as the other  $P_2$  sources with the addition of a large quantity of  $H_2$  that must be pumped in order to maintain ultra high vacuum conditions. Other disadvantages are that the phosphine can not be obtained

with as high purity as the elemental source and it is very toxic.

## 2.0 EXPERIMENTAL

The quaternary layers grown for previous research at Georgia Tech were grown using an InP source, and a great deal of experimental technique was involved in the manipulation of the sources during growth. These procedures are valid when operating in a proof of concept mode and could be repeated to produce quaternary and InP layers in the short term. However, to advance the state of our technology and to reach the long term goals of the program, it was necessary to simultaneously solve the following three problems: The phosphorus source must last at least 30 hrs and longer if possible; there must be real time control of the As and P flux rather than relying on cell temperature; and a means must be devised for coping with the large amount of phosphorus that is introduced into the chamber during growth. The steps that were taken to solve these problems are described in this section.

### 2.1 Phosphorus In The Vacuum System

A significant amount of P is always used to grow MBE InP layers since a high P to In flux ratio is necessary for good quality layers. The background pressure in the MBE system after using the phosphorus source and after the cryopanel has warmed up is typically  $2-4 \times 10^{-6}$  Torr. Phosphorus is the major component of the residual gas in the system at this state and remains so until the system is baked out for at least 6 hours at 120C. The system will then return to  $2 \times 10^{-8}$  Torr and the phosphorus peak disappears.

Several configurations of the vacuum components of the MBE system were tried in order to deal effectively with the P and to maintain UHV conditions. One of the early configurations is shown in figure 1. Large amounts of P deposited in the cryopump required frequent dismanteling and a very messy clean up. There was always enough of the white phosphorus phase present to catch fire unless great care is taken in the cleaning.

The vacuum system arrangement as described above was not satisfactory for dealing with the large quantities of phosphorus evaporated during growth. The arrangement of the cryopump, LN<sub>2</sub>, trap, and valves was changed to the configuration shown in figure 2 and the ion pump was removed completely. Some sacrifice is made in ultimate vacuum with the new configuration, but if the proper procedures for growth and bake out are followed, the system can be operated safely for many growth runs. During growth, the cryopump is open but the liquid nitrogen trap and cryopanel in the growth chamber are filled and the excess phosphorus is trapped on these cold surfaces. After each run, the growth chamber is baked out with the liquid nitrogen trap filled and the interlock valve closed. Excess phosphorus in the growth chamber is converted to red phosphorus by the bake out or moved to the liquid nitrogen trap. After several runs, the liquid nitrogen trap must be cleaned by closing the isolation valve and turning on the phosphorus bake heater to transfer the phosphorus into the liquid nitrogen cooled phosphorus end point trap. In this way the excess phosphorus evaporated in the system is isolated in a safe

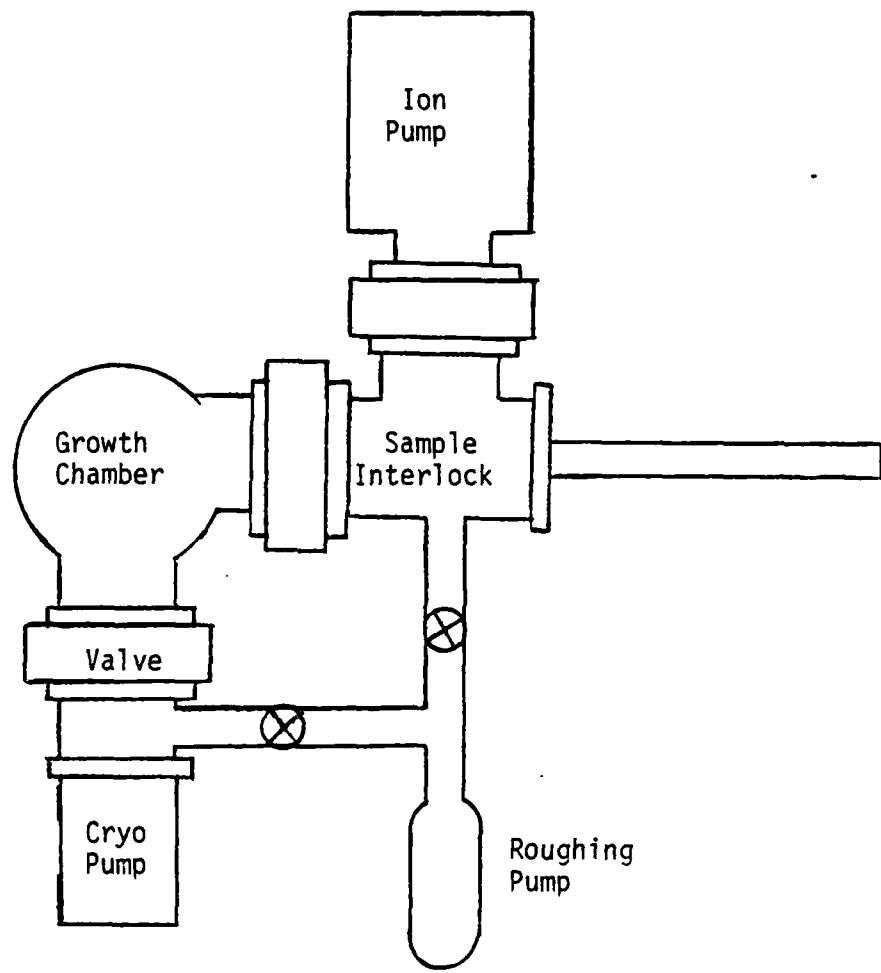


Figure 1. Early Configuration of MBE System.

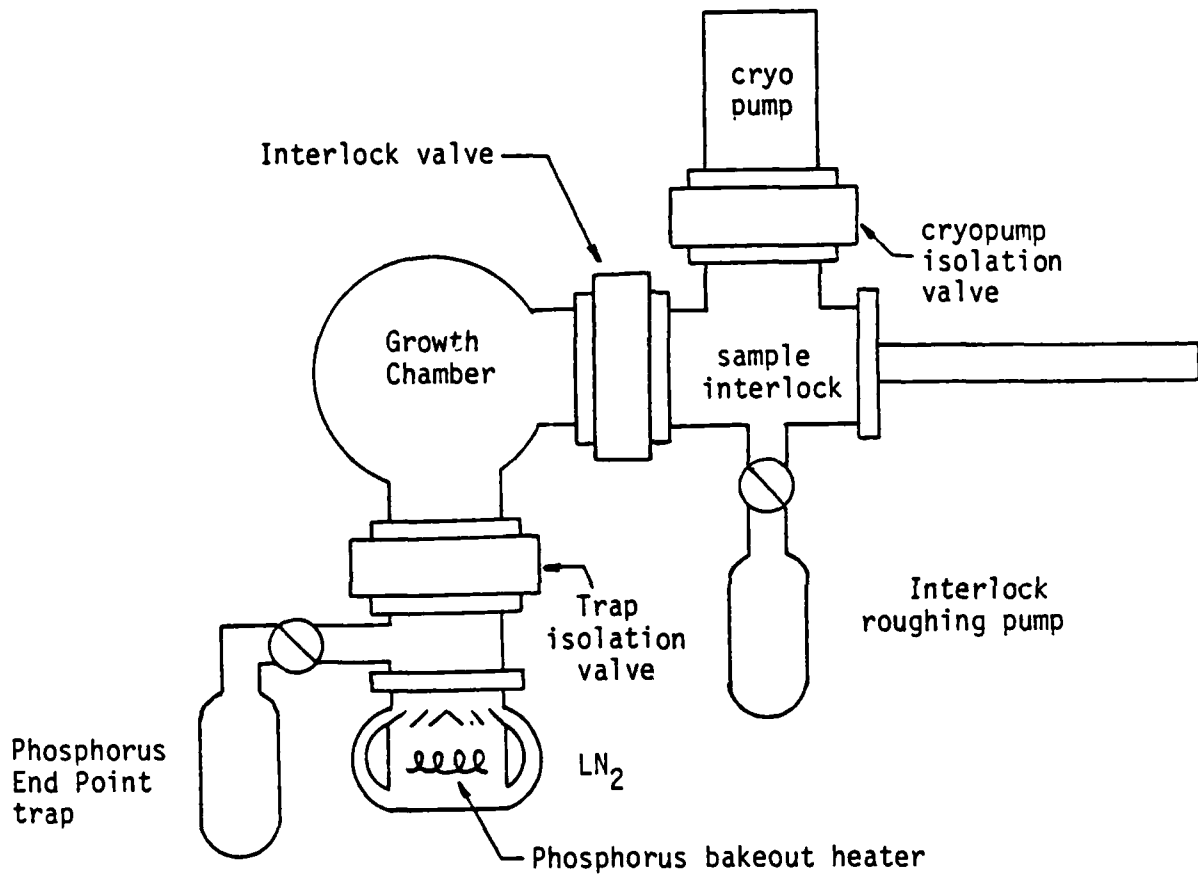


Figure 2. Final System Configuration.

container and can be dealt with as necessary at the proper time. The growth chamber can be opened and the cryopump and liquid nitrogen trap can be removed from the system as necessary without catching fire.

None of the configurations tried thus far worked perfectly. Most of the white P phase can be removed from the system with a moderate 120°C bake but pockets of white P were always buried in the other materials deposited on the cryopanel and cryopump. These pockets smoke and sometimes ignite spontaneously when exposed to air.

Most of what remains in the growth chamber is red P and compounds of P and the other evaporated materials. These materials are very difficult to remove from the system. A very high temperature bake would be required to move them out of the vacuum system. We could not use a bake out temperature higher than 120°C because the cryopump could not function under the extra heat load.

The deposited materials that remain in the growth chamber are also deliquescent. When the chamber is exposed to moist room air all surfaces become covered with a syrupy liquid that continues to accumulate as long as the system is open.

A lot has been learned about dealing with P in the vacuum system but clearly the problem has not been solved satisfactorily. Growth of P compounds has been discontinued in the present system and a new system is being designed and built for future work.

## 2.2 Sources and Flux Monitoring

From past experience it was learned that a  $P_2$  source was preferred for the growth of MBE InP and also the life of the source was significant to consistent production of good layers. For quaternary layer growth, a real time measurement of P flux was necessary to control the alloy composition.

Figure 3 is a drawing of a phosphorus source that was built to evaluate a concept for a cracking source and flux monitor. The source is made of fused quartz and will hold about 20 grams of red phosphorus. There are two exit tubes which are heated internally by a tantalum wire coil. The exit tubes are heated by the internal coil to  $900^{\circ}\text{C}$  to crack the  $P_4$  molecules to  $P_2$ . One exit tube is directed at the substrate and provides the  $P_2$  flux for growth. The other exit tube is directed towards a nude ion gauge where the pressure or  $P_2$  flux can be measured at all times during growth. Part of the source concept was to use the analog output from the ion gauge control unit to control the phosphorus source temperature giving real time flux control during growth.

Several unintentionally doped InP layers were grown to evaluate the performance of this phosphorus source. The 20 grams of phosphorus provided about 10 hrs of growth time at 1.0 micron per hour growth rate which is a phosphorus consumption of about 2 gms per hour.

The effluent flux from the phosphorus source was measured with a UTI mass spectrometer. As the temperature of the exit tube was increased, the  $P_4$  component of the beam decreased until the

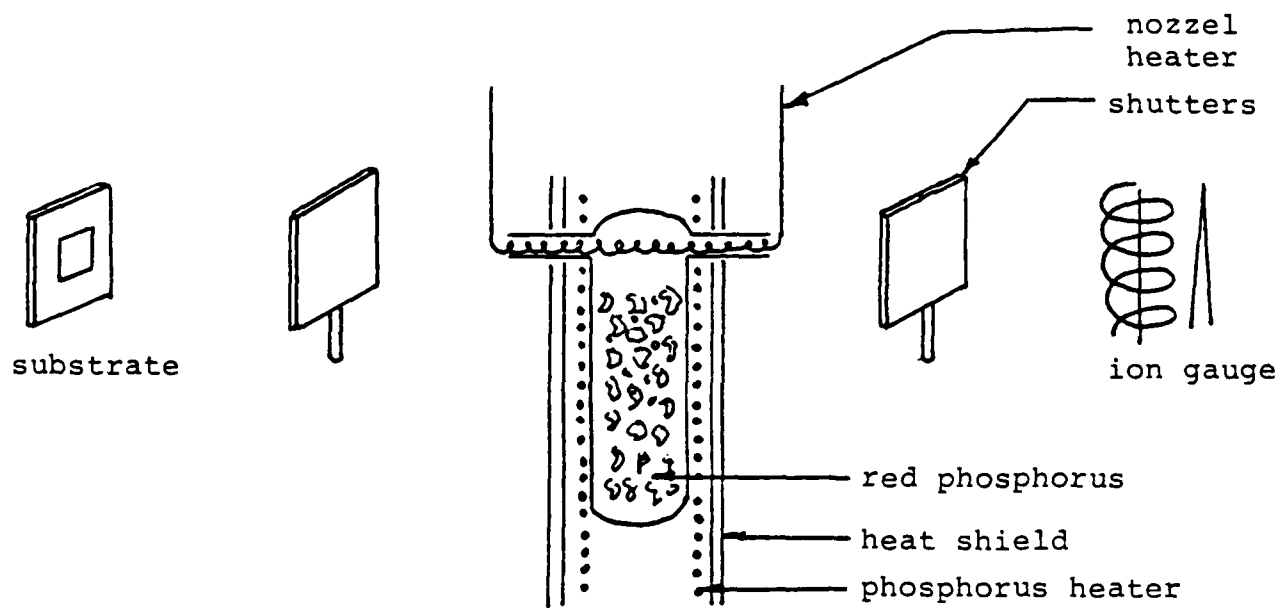


Figure 3. Phosphorus ( $P_2$ ) source with ion gauge flux monitor.

$P_4$  peak is less than 0.2% of the  $P_1$  or  $P_2$  peaks. The temperature of the exit nozzle could be increased, but there is a danger of the quartz tube becoming a doping source, so the temperature was limited to 900C.

This evaluation of the cracking source with flux monitor was encouraging. The cracker worked well and the source lasted longer than any other P source previously tested. However, as the source was configured in figure 3, changes in the source flux could not be separated from changes in growth chamber vacuum.

Larger sources were then made for P and As using the same cracker and flux monitor concept. The flux monitor was improved as shown in figure 4. These sources hold 125 grams of P or As and each source has two nozzles; a 6 mm diameter growth flux nozzle and a 1.0 mm diameter flux monitor nozzle. The nozzles are heated by an internal Ta wire coil and the flux monitor nozzle is directed into a small LN<sub>2</sub> cooled chamber that contains the monitor ion gauge.

Twenty InP layers were grown with the new phosphorus source for a total operation time of at least 40 hrs, including an hour of operation in calibrating the flux before each run. When the phosphorus source was checked after these runs, it was found to be 80% full. The longevity of these new sources thus seems to be satisfactory for the growth of good MBE material.

The large size of the source increases the source lifetime but also increases the response time to temperature adjustments for flux changes. At least an hour of source operation is

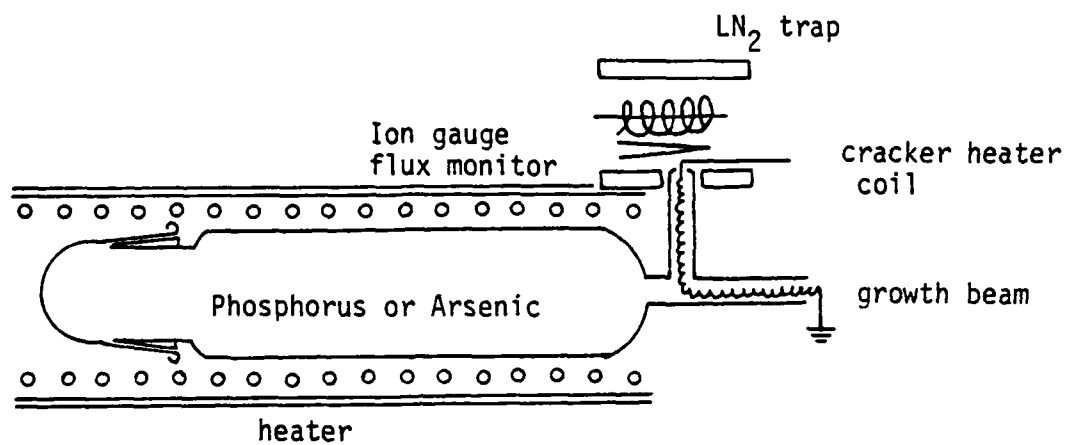


Figure 4. New large arsenic and phosphorus sources with cracker and flux monitor.

required to bring the source to equilibrium at the particular flux level required. The flux from the source is also measured at the end of each run to record changes that may have occurred during the growth. These values measured after the run are plotted vs oven temperature in figure 5 with points numbered in time sequence. Points 2 through 12 fall close to the straight line drawn in the figure with latter runs 13 to 16 falling generally below in the line indicating a gradual change in the characteristics of the source with time. Keeping track of this aging is important in setting the temperature of the source to achieve the equilibrium conditions that are necessary for uniform quaternary films.

Changes in the arsenic or phosphorus flux can be observed during growth with the flux monitor ion gauges. Adequate runs have been made using these gauges to give confidence that they can be useful in measuring the flux during the run. Care must be exercised to insure that the  $\text{LN}_2$  traps in the system remain fully charged at all times because changes in the background pressure also register on the flux monitor gauges. The monitor gauges are useful in measuring the flux but the long term stability is not sufficient for the reliable flux control that is needed for quaternary layers. Perhaps some improvement in the flux monitor could be made by adjusting the aperture to establish the magnitude of the control flux at about one order higher than the desired growth flux at the sample. A higher control flux should make the monitor less sensitive to background pressure changes.

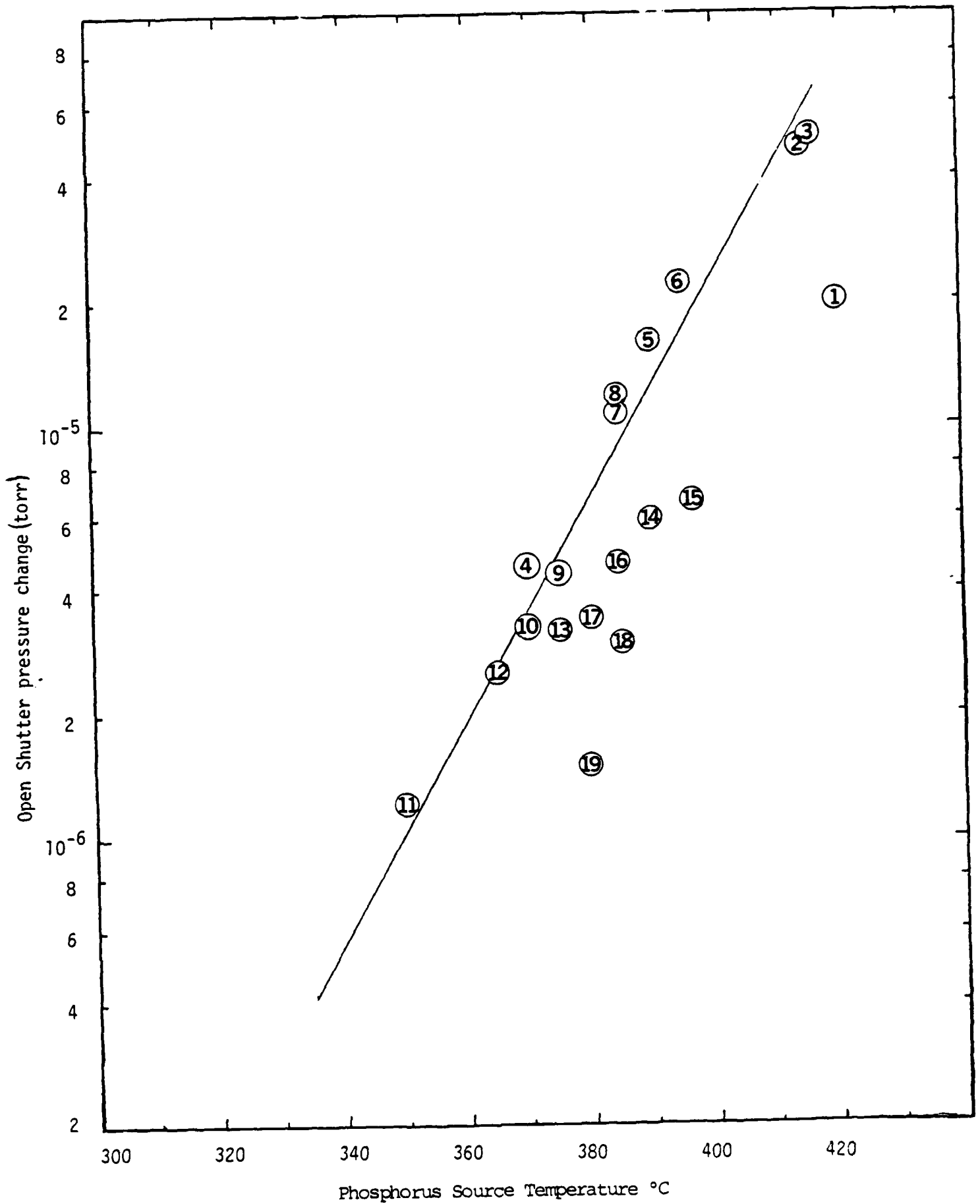


Figure 5. Dependence of Phosphorus Pressure on Phosphorus Source Temperature.

The relation between the flux at the monitor and the flux at the sample should be linear; thus, high monitor pressure should not obscure small changes in flux at the sample.

### 3.0 MATERIAL GROWTH AND CHARACTERIZATION

#### 3.1 InP Layers- "T CELL"

Eight InP layers were grown using the "T cell" red phosphorus cracking source shown in figure 3. Substrate temperatures of 400, 500, and 520C have been utilized with phosphorus to indium flux ratios between 4 and 25. The best surface was grown to 500°C with a flux ratio of 25. All of the layers were not evaluated because the layers grown at low flux ratios had poor surfaces. Photoluminescence and electrical measurements were made on the thickest layers with the best surfaces.

Measurements of the carrier concentration and mobility were taken for sample temperatures between 150 and 200K using the Van der Pauw technique. These measurements showed that both of the samples measured were n-type with electron concentrations in the mid  $10^{14}\text{cm}^{-3}$  range at 300K. However, as shown by Figures 6 and 7, the electron concentration decreases rapidly on cooling and becomes less than  $10^{13}\text{cm}^{-3}$  below 150K. The electron mobility is found to be almost independent of temperature in this range with values of  $1800\text{ cm}^2/\text{Vs}$  and  $1000\text{ cm}^2/\text{Vs}$  for samples F1118 and F1130 respectively. As a consequence of these properties and the layers thicknesses, the sample resistance becomes greater than 50 Megohms below 175K, making it difficult to obtain accurate data with our automated Hall effect apparatus.

The low mobility values indicate that the sample is heavily compensated. An estimate of the ionized donor impurity

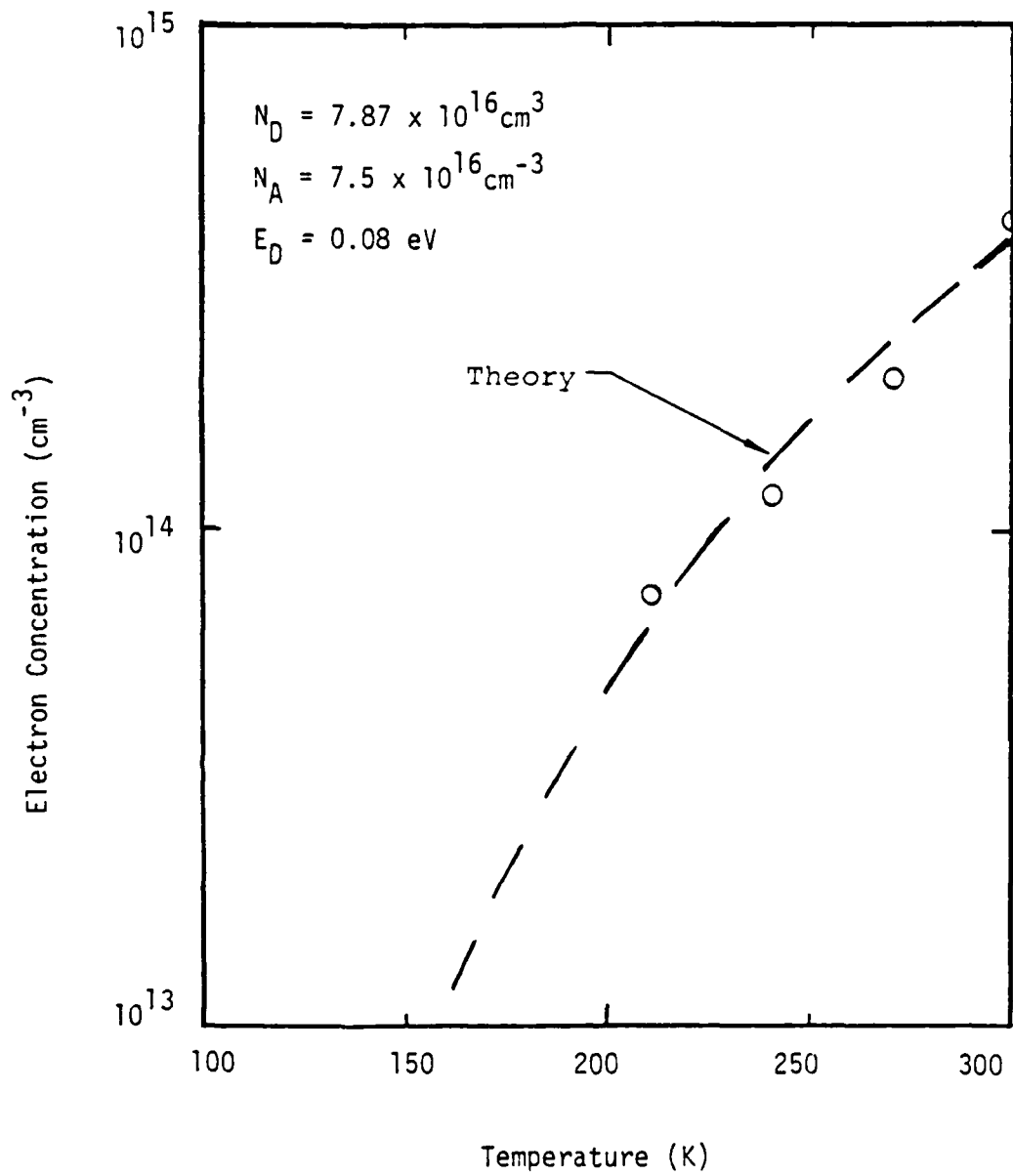


Figure 6. Dependence of electron concentration on temperature for InP sample F1118.

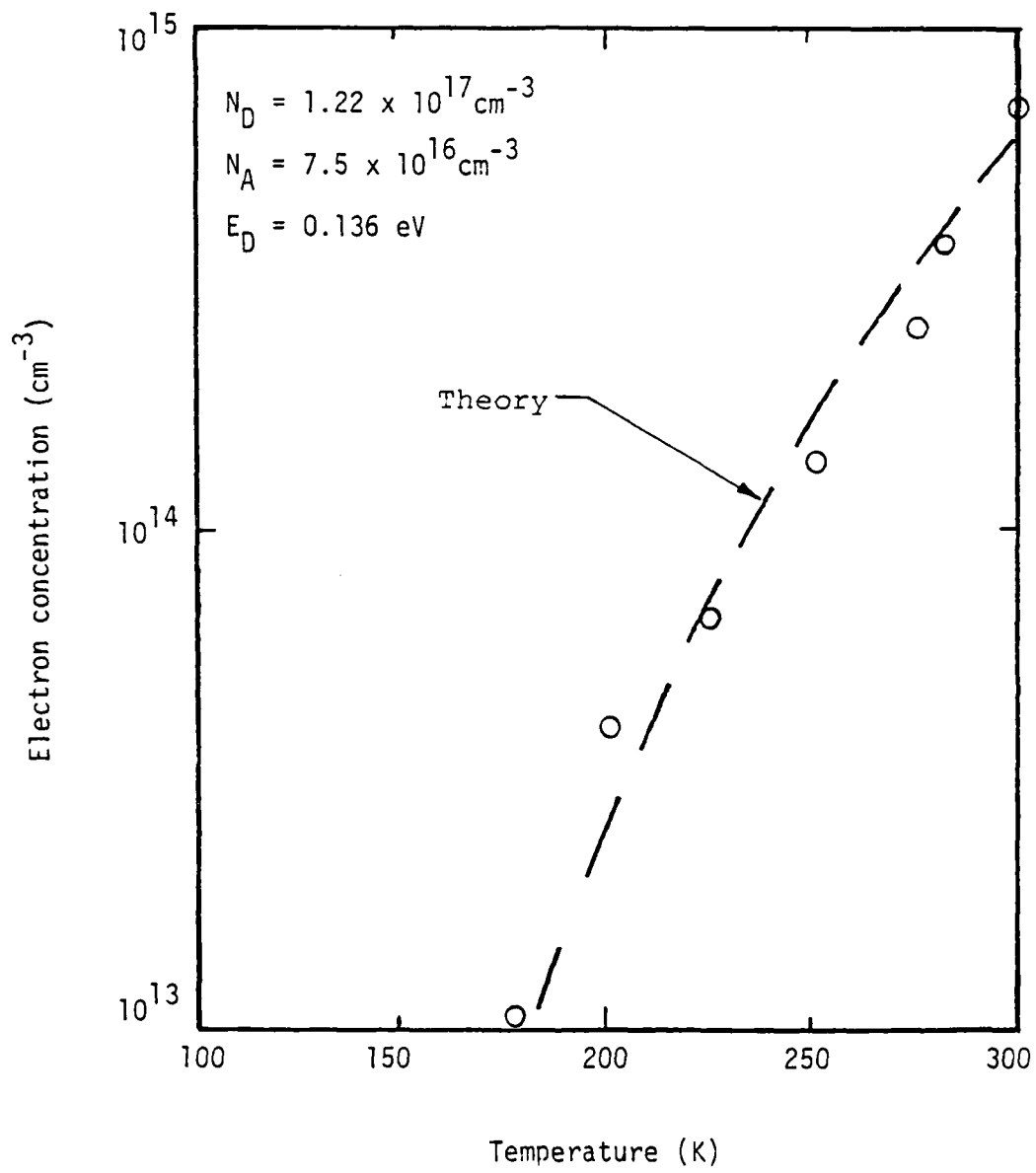


Figure 7. Dependence of electron concentration of temperature for InP sample F1130.

concentration has been obtained from Rode's analysis<sup>12</sup> and is found to be  $10^{17} \text{ cm}^{-3}$ . Estimates of the donor,  $N_D$ , and acceptor,  $N_A$ , concentrations and the donor ionization energy,  $E_D$ , were also obtained from the temperature dependence of the electron concentration. For nondegenerate compensated semiconductors, these quantities are related by the expression:

$$\frac{n(N_A - n)}{N_D - N_A - n} = \frac{N_C}{2} \exp\left(-\frac{E_D}{kT}\right)$$

where  $n$  is the measured electron concentration at temperature,  $T$ , and  $N_C$  and  $k$  are the density of states in the conduction band, and Boltzmann's constant, respectively. To obtain starting values for this expression,  $E_D$  was estimated from the dependence of  $n$  on  $T$ , and a value for  $N_A$  was estimated from the mobility data. The values of the parameters  $N_D$ ,  $N_A$  and  $E_D$  were then adjusted to give the best fit to the data as shown in the figures. From this fit the material parameters can be estimated to 15%. This analysis confirms that the samples are heavily compensated with donor and acceptor concentrations near  $10^{17} \text{ cm}^{-3}$  and donor levels at 0.08 and 0.136 eV below the conduction band. The reason for the difference in the donor ionization energies is not known but could be related to the fact that sample F1130 was grown at a lower  $P_2/\text{In}$  ratio than sample F1118.

The optical quality of the samples was investigated using 77K photoluminescence measurements. The samples were illuminated

by a 6 mW He-Ne 6328<sup>0</sup>A laser, and the photoluminescence was detected in reflection at 30<sup>0</sup> off normal incidence using a 1/2-m monochromator and a Hamamatsu R9543-02 PMT. The spectral resolution was better than 0.3 meV. The photoluminescence spectra taken for samples F1110, F1118 and F1130 are shown in Figures 8, 9 and 10 respectively. All spectra show a single peak centered at 1.418 eV corresponding to emission resulting from band-to-band recombination. The half-widths at half-maximum of these features are observed to be very narrow (6-8 meV) for these sample temperatures, indicating good quality material. The differences in the PL peak intensities are believed to be related to the sample thicknesses and growth conditions. Samples F1110 and F1118 were grown under very similar conditions and therefore are expected to have similar properties. The large difference in their PL response is therefore attributed to the fact that a large portion of the photon-excited carriers in the thinnest sample will recombine non-radiatively in the substrate thus making no contribution to the photoluminescence. Following this argument, one would expect that the thickest sample, F1130, would have the largest PL response. However, the sample was grown under a reduced P<sub>2</sub>/In ratio (12 as opposed to >25 for the other samples) and thus its properties differ. For example, the electrical characterizations indicate a deeper donor level for this layer than for F1118.

The results of the materials characterization indicate that the properties of MBE grown InP appear to improve for higher

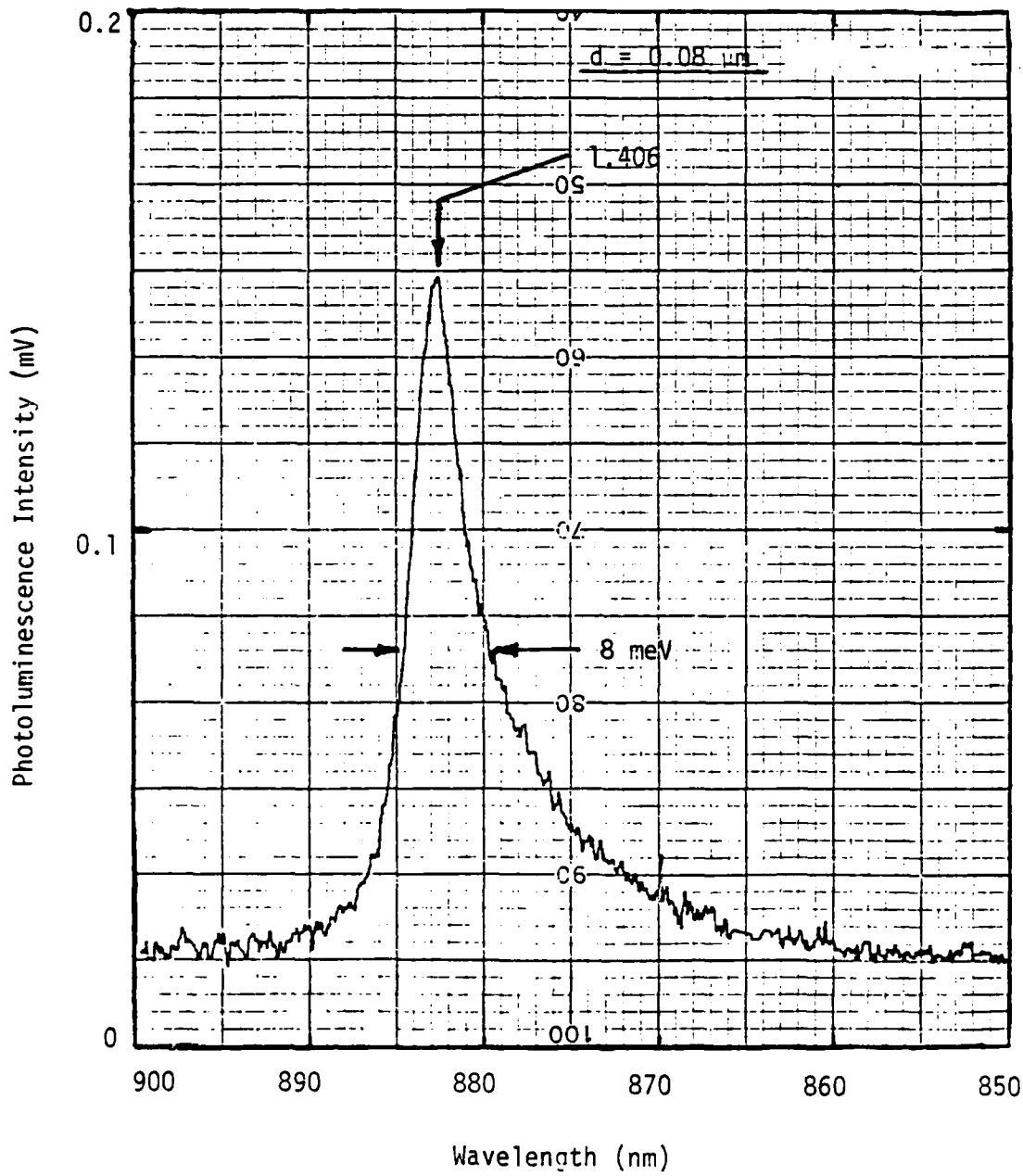


Figure 8. Photoluminescence spectrum of InP sample F1110 at 77K.

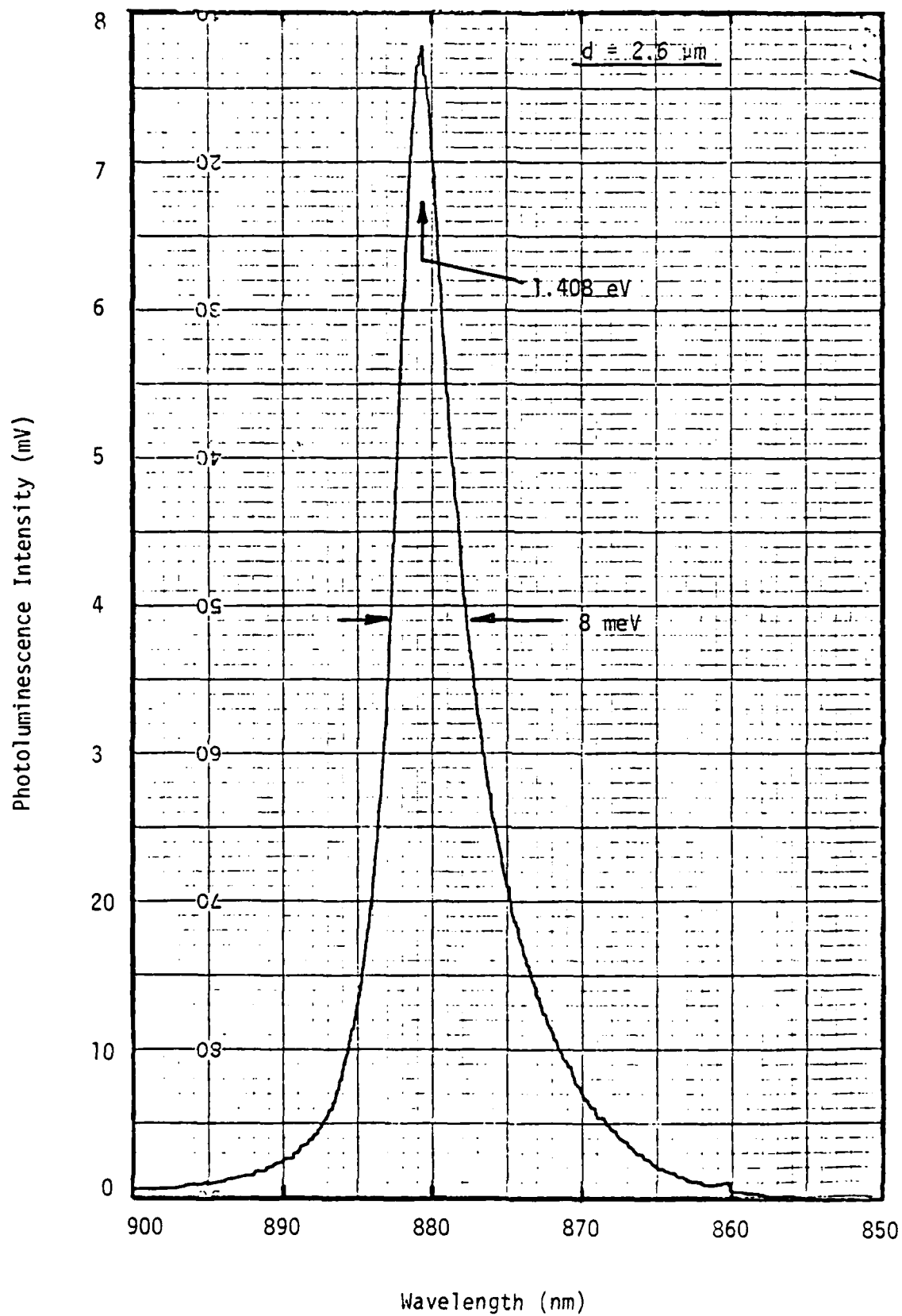


Figure 9. Photoluminescence spectrum of InP sample F118 at 77K.

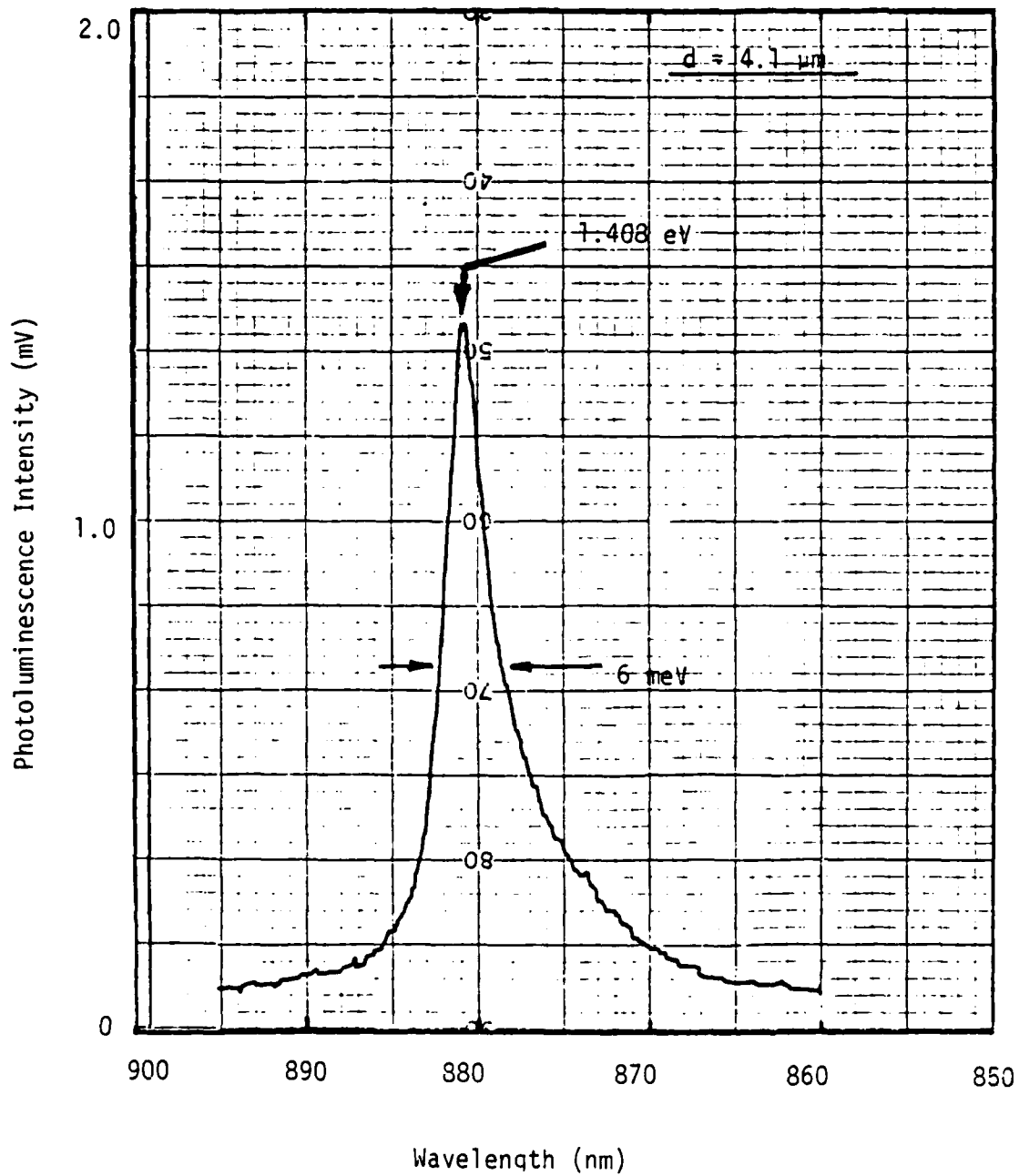


Figure 10. Photoluminescence spectrum of InP sample F1130 at 77K.

P<sub>2</sub>/In ratios and higher substrate growth temperatures. Both of these developments stress the need for a larger and, if possible, a more efficient P-source.

### 3.2 InP Layers - 125 gram source

More than twenty InP layers were grown using the 125 gram source as shown in figure 4. The first three layers had good surfaces and good room temperature mobility. Many attempts were made to reproduce these layers, but all failed because of poor surfaces until the current in the cracker nozzle was increased from 5.5 to 7.5 amps. The reason for this change in growth conditions is not known. It may be speculated that a small part of the new red phosphorus material consisted of a metastable phase of phosphorus that evaporated as the P<sub>2</sub> molecular species and was evaporated in the first three runs or converted by heating to the normal red phosphorus phase.

The mobility at room temperature was measured to be 4,060 cm<sup>2</sup>/vs for the best sample grown at 480C and is the highest that we have found reported in the literature for MBE material. The mobility follows a T<sup>-2</sup> line between 200 and 300K as reported by Glisksman and Weiser<sup>14</sup> for bulk material. Below 200K the mobility exhibits an anomalous behavior that would indicate compensating impurities or defects in the crystal order. The oriented surface defects discussed in the next section certainly indicate crystal defects in the layers. If this anomalous temperature dependence of the mobility persists in future layers, SIMS profiles will be made on the layers to identify the impurities that may be

present.

The samples grown were all n-type with the lowest carrier concentration of  $1.3 \times 10^{16} \text{ cm}^{-3}$  measured on samples grown at 480C. A carrier concentration 2-3 times higher was consistently obtained on samples grown at 430C. If the inverse relationship between carrier concentration and substrate temperature continues at higher substrate temperatures we should obtain a carrier concentration of mid  $10^{15}$  at 580C.

The optical quality of the samples was investigated using 77K photoluminescence measurements. The spectral resolution was better than 0.3 meV. The photoluminescence spectra taken for samples grown at 480 and 430C are shown in Figure 11. All spectra show a single peak centered at 1.418 eV corresponding to emission resulting from band-to-band recombination. The full widths at half-maximum of these features are observed to be 9.6 and 12.7 meV respectively for these growth temperatures, indicating good quality material. The differences in the PL peak intensities are believed to be related to the crystal quality of the layers since the layer grown at 480C was thinner and less heavily doped than the layer grown at 430C but still shows a higher and sharper PL peak.

It would be worthwhile to spend enough time growing InP layers to better understand the process and determine the limits of substrate temperature and In to P flux ratio for the best quality layers. However, since the program was behind schedule and the last layers grown had excellent surfaces and room

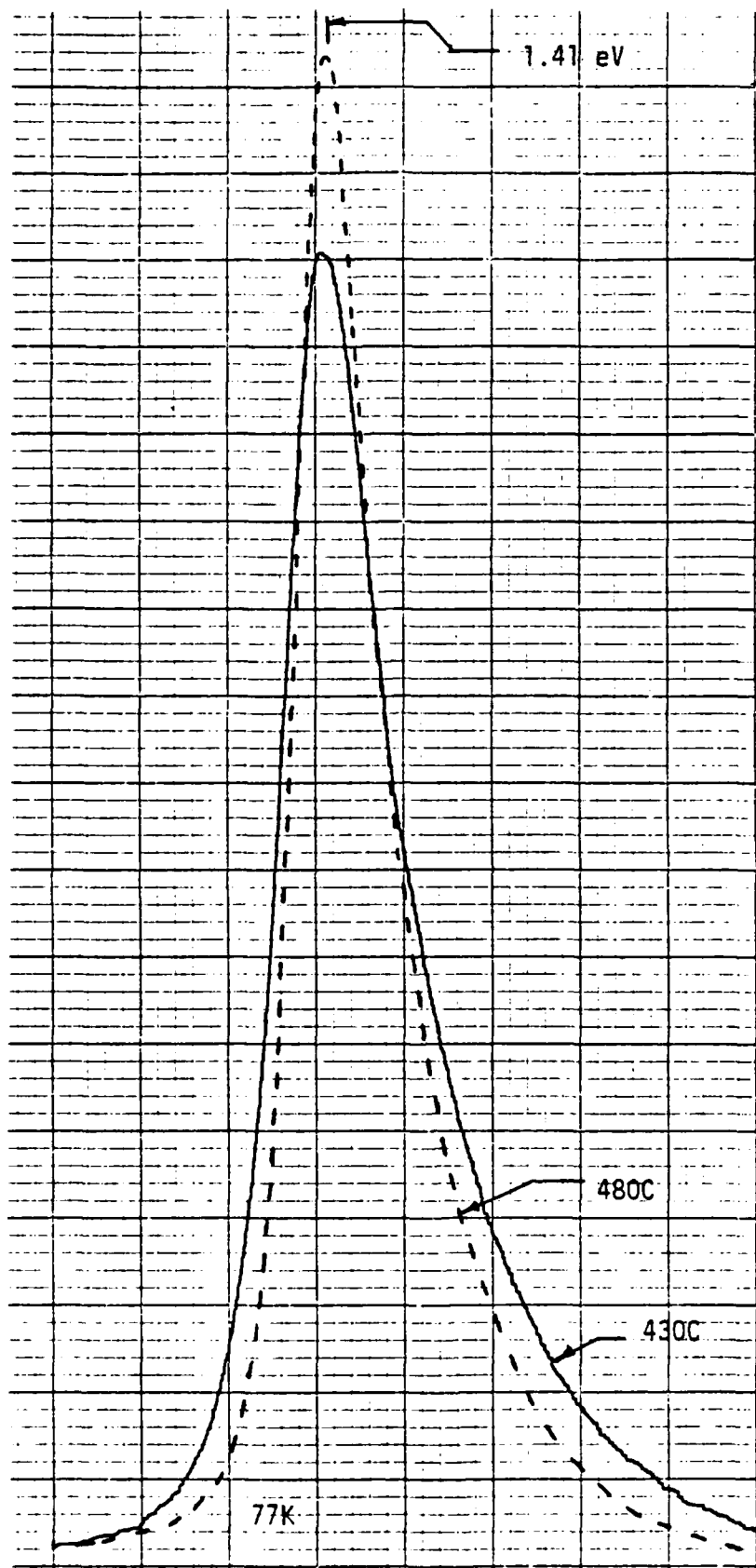


Figure 11. Photoluminescence for films grown at 430 and 480C.

temperature mobility, work proceeded immediately to the growth of quaternary layers.

### 3.2 Surface Features

A common surface problem has been observed in the growth of MBE InP layers with all of the phosphorus sources described above. Figure 12 is a photomicrograph of a typical surface grown at Georgia Tech with cracked red phosphorus. Also shown is a profile of one of the surface features that shows a triangular cross section that starts 200A below and rises 550A above the average surface. The same features are reported by Chow<sup>8</sup> using a phosphine source, Asahi<sup>9</sup> using red phosphorus, and Meeks<sup>11</sup> using an InP source. A common orientation of the long dimension of the features in the (011) direction is observed<sup>9</sup>.

The origin of the surface features is not known; neither does it seem to be (thus far) associated with either good or bad mobility of the material. It had been noted in the past that symmetrically cut square Hall samples with ohmic contacts at the corners showed a consistent asymmetry in the resistivity measurements. Directional differences in resistivity of 100% or more have been observed. Special Hall samples with contacts at different angles with respect to the surface features were prepared to determine if the asymmetry in resistivity could be associated with the surface features. Thus far, the measurements show no such association. Asahi<sup>9</sup> reports that the number of features can be reduced by increasing the  $P_4/In$  ratio but the features are still present at a ratio greater than 100.

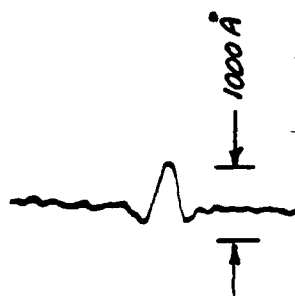
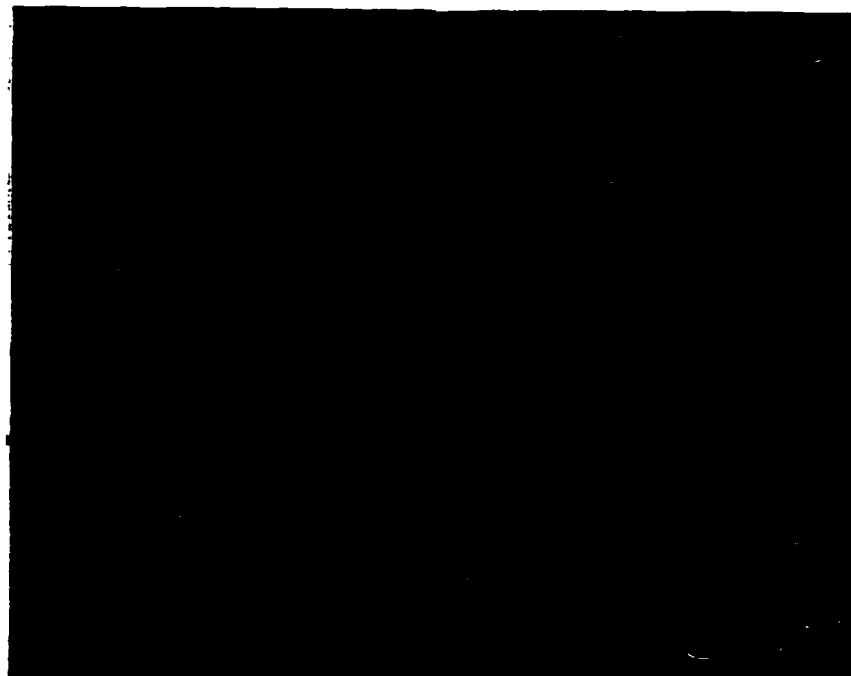


Figure 12. Photomicrograph of InP MBE surface and profile of a typical surface feature.

The substrate temperature effects the formation of the elongated surface features and the electrical properties. Figure 13 shows phase contrast optical micrographs of typical surfaces grown at 430 and 480C with a phosphorus to indium flux ratio of 20. The surface of the layer grown at 430C does not show any of the elongated surface features that can be seen on the 480C sample.

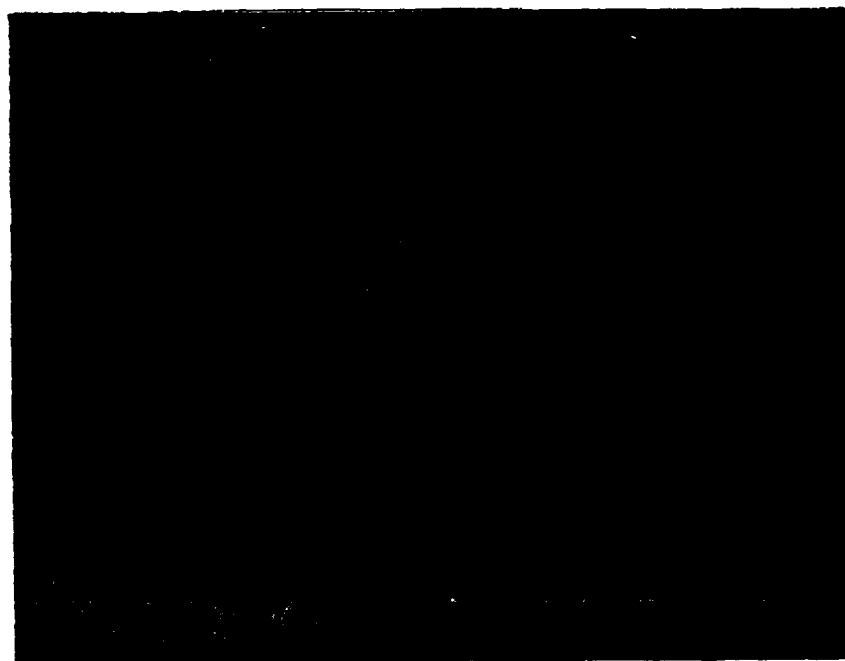
At the lower substrate temperature, these features are no longer present but, as can be seen from Figures 14 and 15, the electrical properties are not as good for the lower temperature films. This is consistent with the results of Norris & Stanley<sup>13</sup> who report mobilities of films grown at 150, 300 and 380C.

#### 3.4 Quaternary Layer Growth

Table 1 lists the quaternary layers grown with the growth parameters and composition as obtained by electron microprobe. The x and y values and lattice constant determined from these measurements are also listed in table 1 and used to plot the numbered points in figure 16. The points are numbered points and sample numbers is given in table 1. Figure 16 also shows the target value of  $x = 0.37$  and  $y = 0.83$  corresponding to a wavelength of 1.55 microns with lattice match to InP. Sample G0627 (Point 7) has the composition to closely match the InP substrate but faulty operation of the In source shutter caused this layer to be polycrystalline. Two other samples G0628 and G0629 (points 8 & 9), with growth conditions very close to 7, had different compositions indicating different sticking coefficients



430C



480C

Figure 13. Phase contrast micrographs of layer surfaces grown at 430C and 480C 500x.

# ELECTRON MOBILITY OF INP

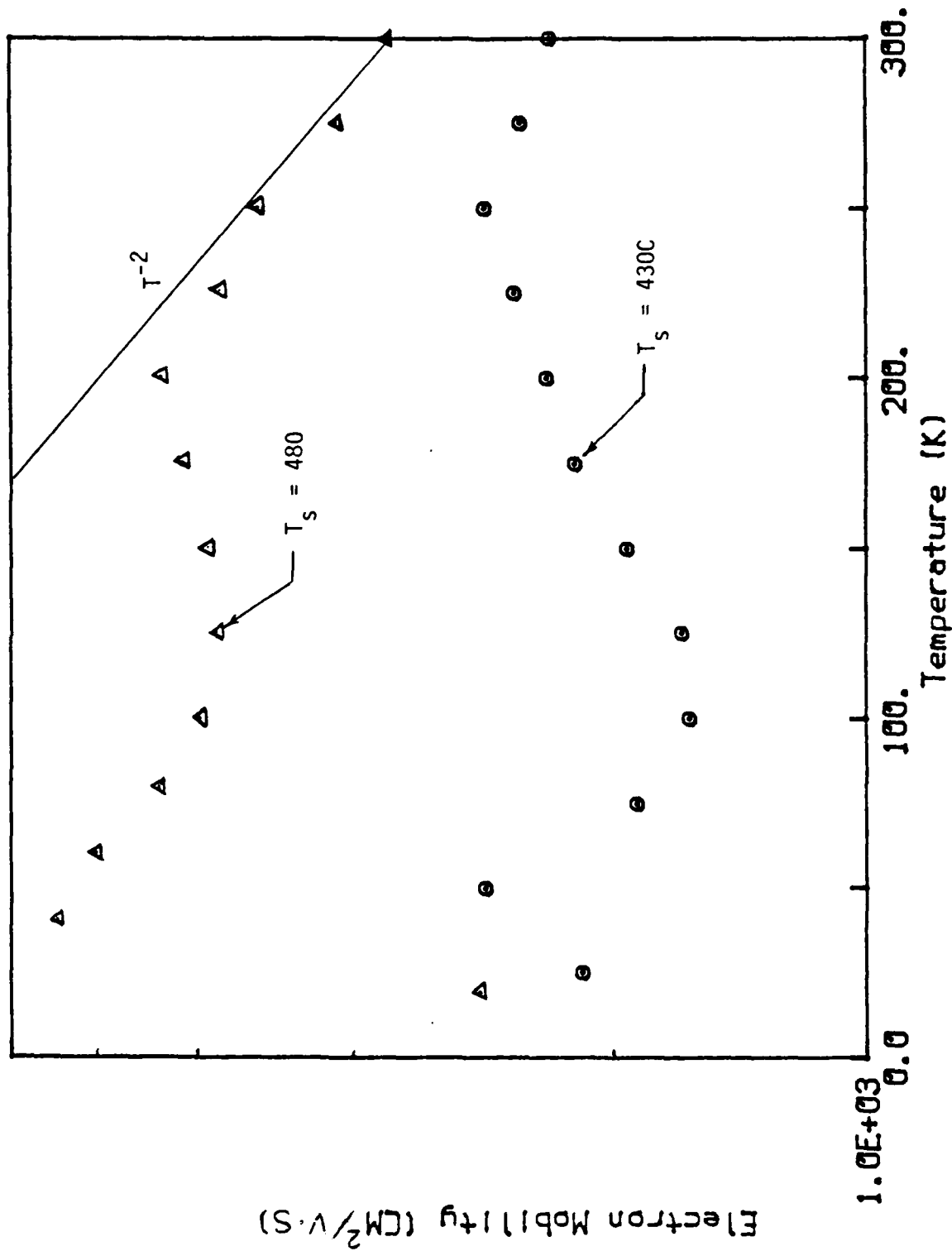


Figure 14. Mobility for T<sub>s</sub> = 430 and 480C.

# ELECTRON CONC. OF INP

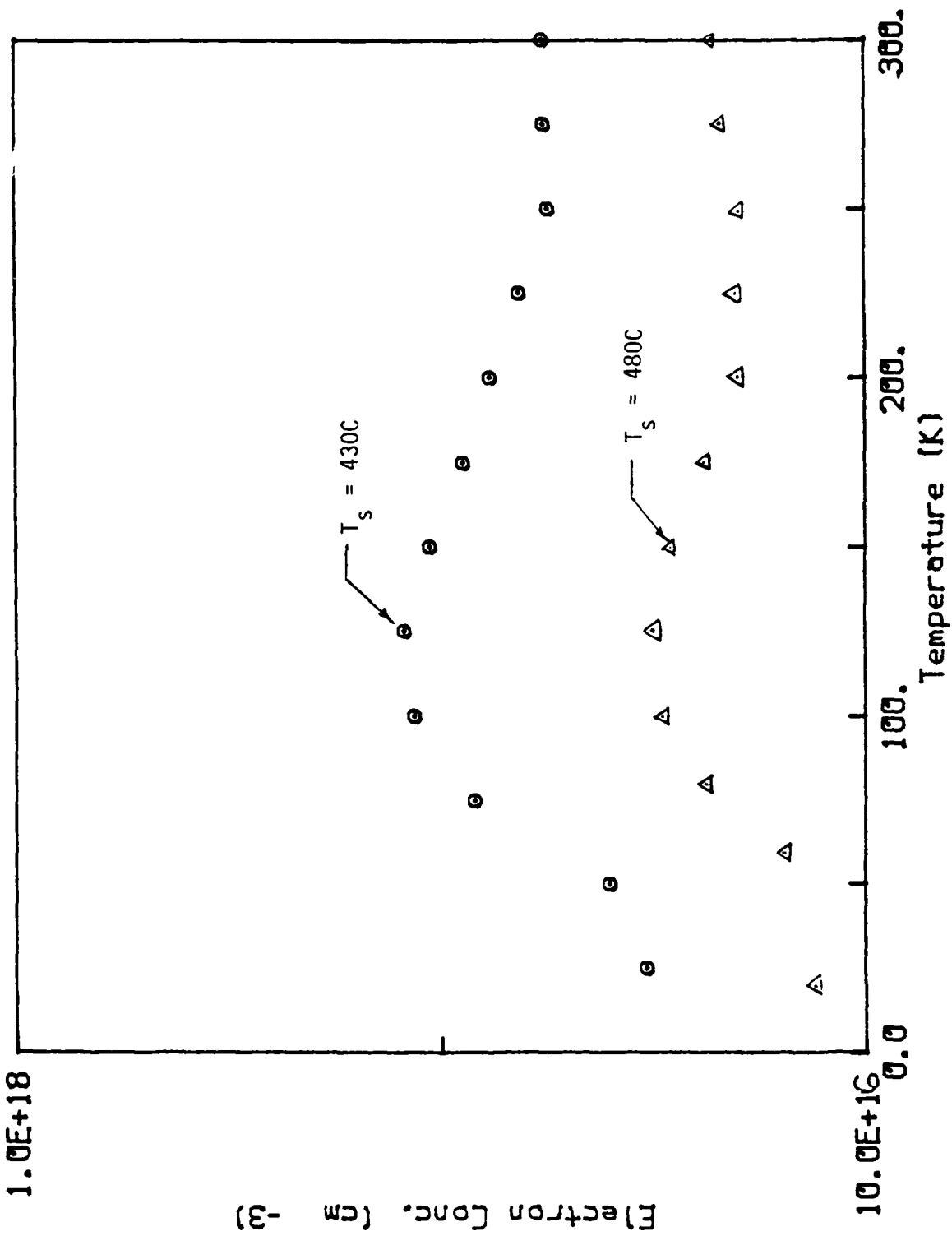


Figure 15. Electron concentration for  $T_s = 430$  and  $480C$ .

Table 1. Quaternary Layers with Growth Conditions and Composition Results.

Sample	Fig 4	Temperature				Composition*								x-ray A <sub>O</sub>	thick μm	rate μ/hr
		In	Ga	As	P	In	Ga	As	P	X	Y	Comp A <sub>O</sub>				
G0522	1	820	940	380	380	.198	.402	.222	.178	.66	.56	5.71	3.9	2.39		
G0524	2	810	950	380	385	.152	.493	.172	.183	.76	.48	5.66	4.85	2.08		
G0529	†	830	930	380	380	-	-	-	-	-	-	-	-	-		
G0612	3	820	920	380	380	.274	.254	.262	.209	.48	.56	5.78	3.7	3.89		
G0613	4	820	900	385	385	.265	.263	.265	.208	.50	.56	5.77	8.8	4.4		
G0614	5	820	900	390	380	.271	.259	.259	.211	.49	.55	5.77	3.9	3.9		
G0615	†	820	900	395	390	-	-	-	-	-	-	-	-	-		
G0620	6	820	900	399	393	.256	.273	.270	.201	.52	.57	5.76	6.6	3.25		
G0627	7	820	875	410	390	.286	.177	.419	.118	.38	.78	5.85	2.4	3.6		
G0628	8	820	865	410	385	.310	.213	.242	.235	.41	.51	5.79	2.3	2.3		
G0629	9	820	865	411	390	.243	.220	.343	.194	.47	.64	5.69	2.7	2.7		

\*Composition by electron microprobe.

†Metallic drops on surface.

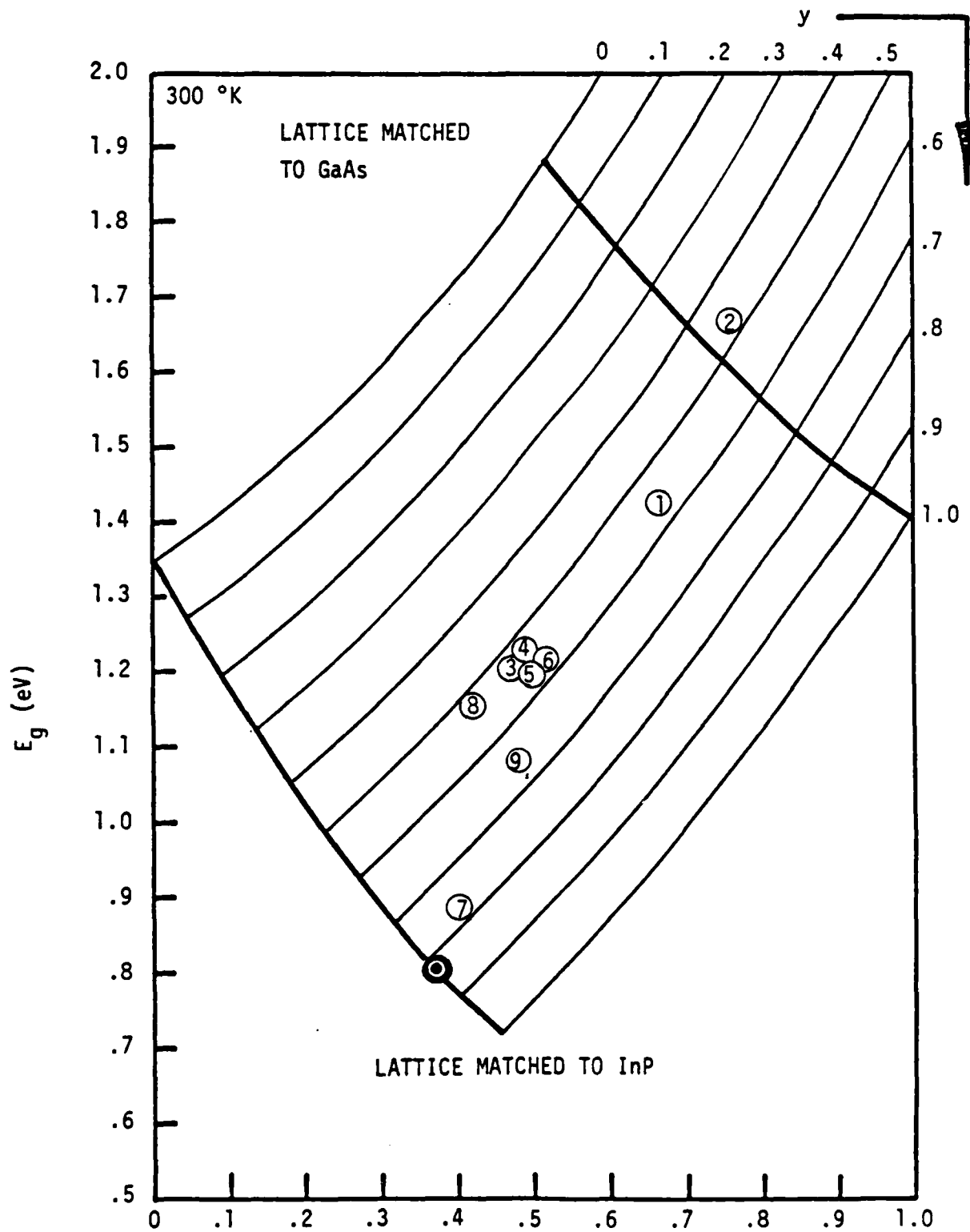
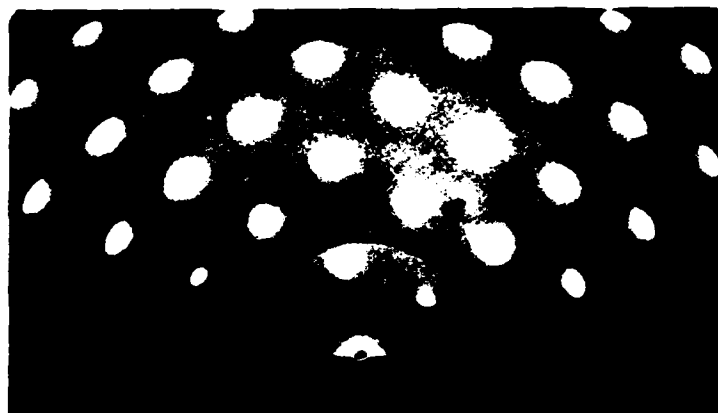


Figure 16. Lattice Match Data for  $\text{In}_{1-x}\text{Ga}_x\text{As}_y\text{P}_{1-y}$  Layers.

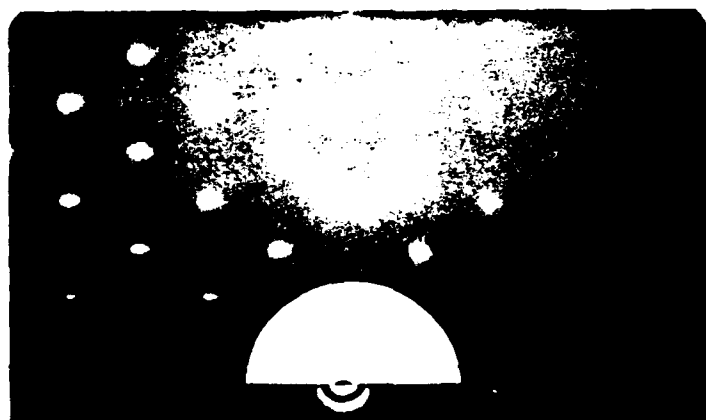
for the alloy components on single crystal or polycrystalline surfaces.

It can be seen in figure 16 that samples G0524 and G0628 are respectively the poorest and best latticed matched layers. Thus, for the clearest definition of differences, most of the evaluations of this material have been performed on these two samples. And, since the best sample still has a lattice mismatch of 1.0%, a complete evaluation of the other layers between these two would add little information.

Reflection high energy electron diffraction (RHEED) patterns were taken on samples G0524 and G0628 and are shown in figure 17. From figure 16, it can be seen that G0524 was not well lattice matched to the InP substrate. In fact, the composition of this layer was such to provide a good match to GaAs. The poor lattice match is confirmed by the RHEED pattern (figure 17a) for this layer. The clear spot pattern indicates highly ordered growth but the large size of the spots confirm that the layer is not single crystal. When Hall measurements were attempted on this layer, the contacts were all highly rectifying. This also indicates a high resistivity layer of poor crystal quality. The RHEED pattern for sample G0628 (figure 17b) is much better but is still not as good as the pattern obtained on the substrate material (figure 17b). The pattern is very clear and the spot size is much smaller than those in 17a, but the spots are elliptical and there are no Kicuchi line features as seen in the substrate pattern.



(a) G0524



(b) G0628



(c) InP Substrate

Figure 17. Reflection High Energy Electron Diffraction Patterns of Quaternary Layers and InP Substrate.

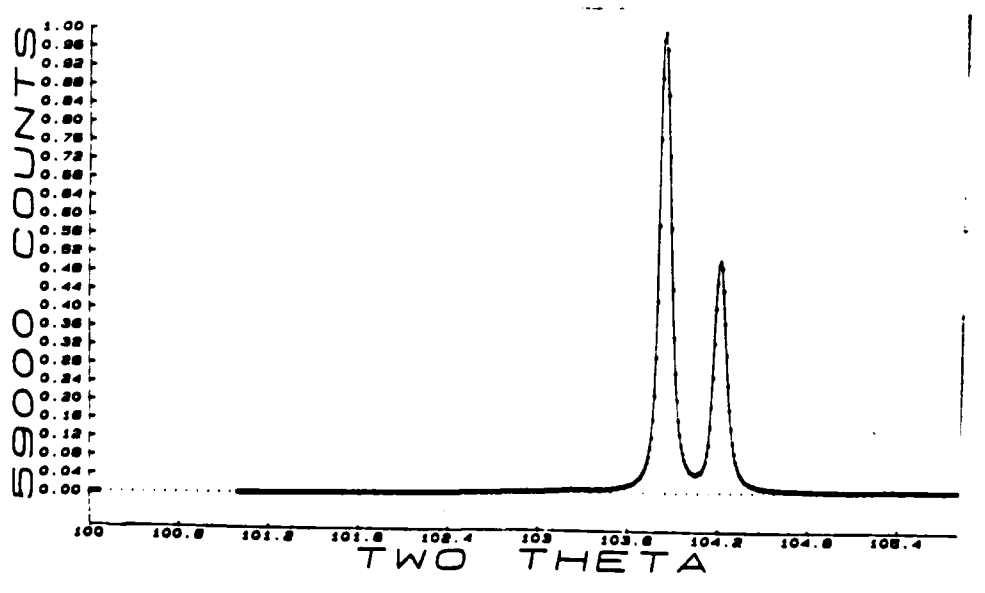
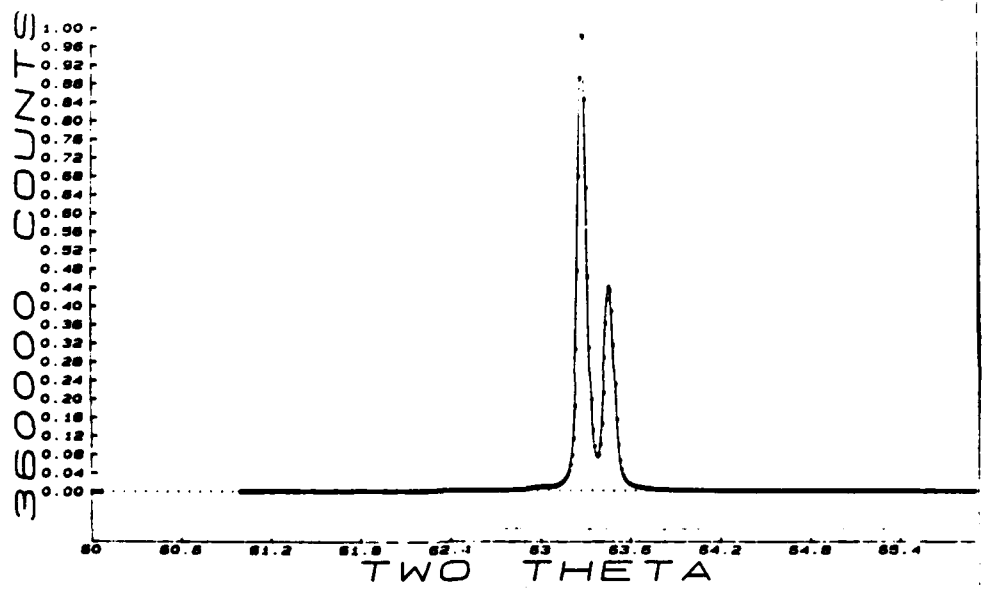
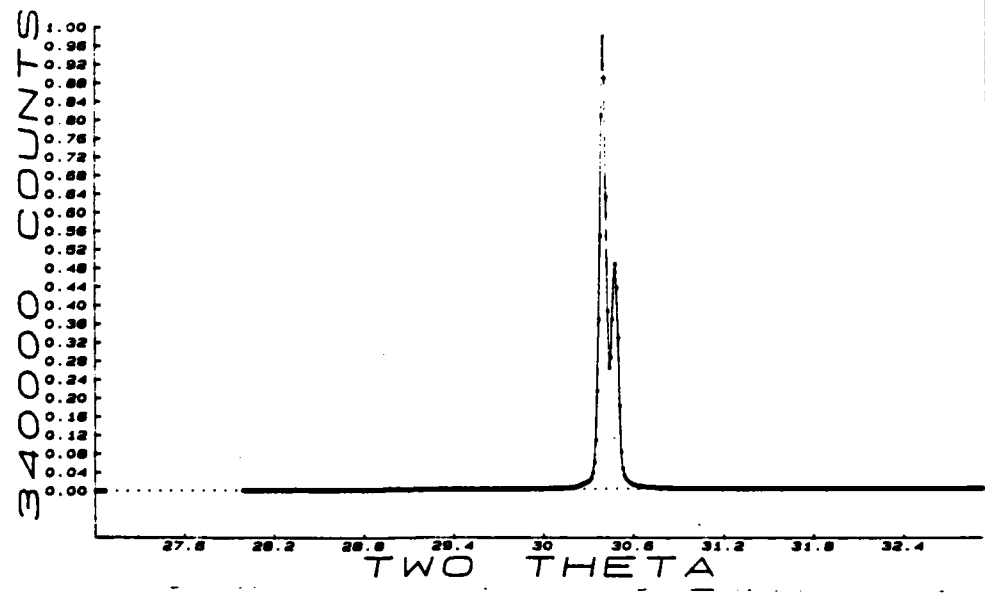


Figure 18, X-ray diffraction peaks for InP substrate.

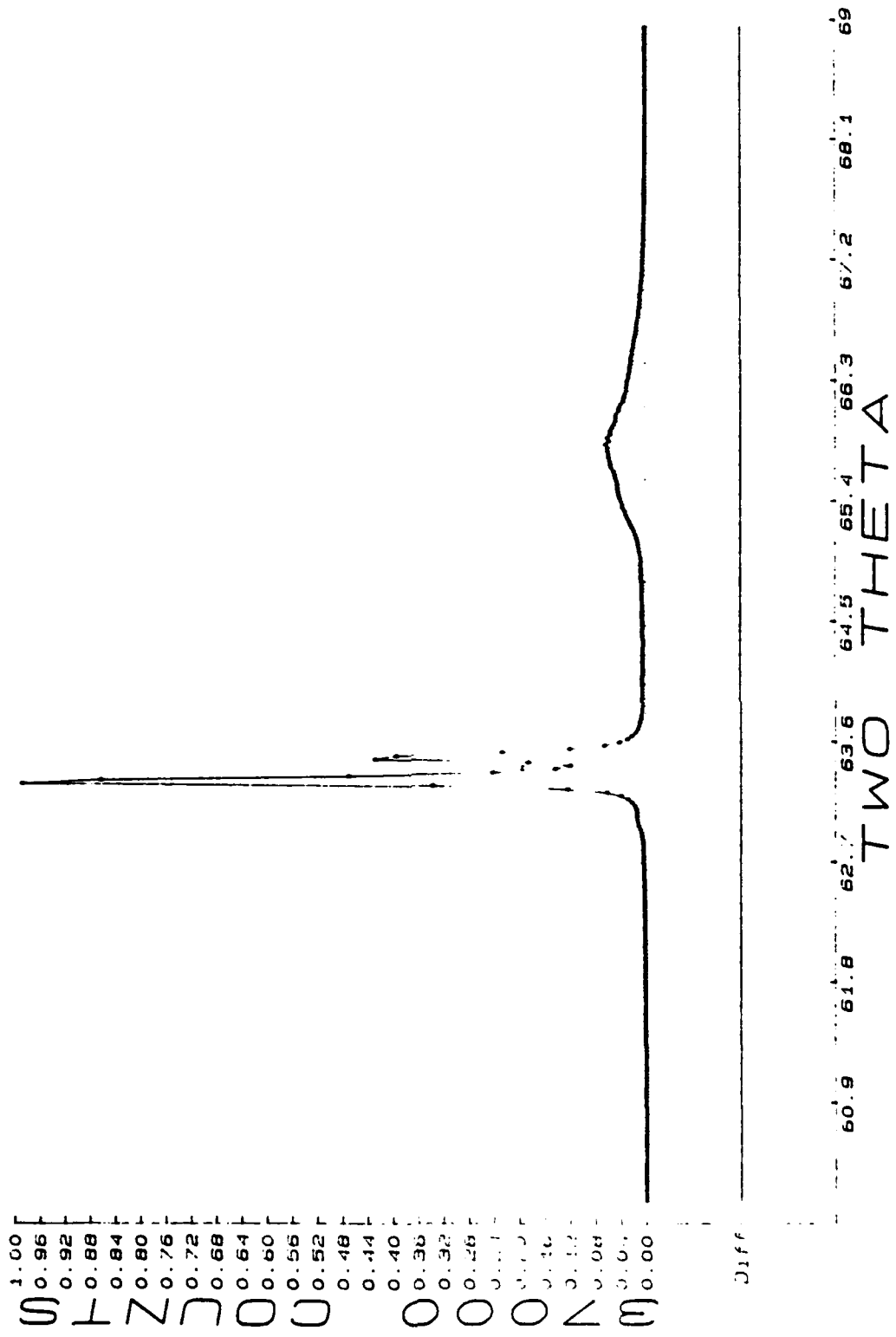


Figure 19. InP substrate with quaternary layer G0524.

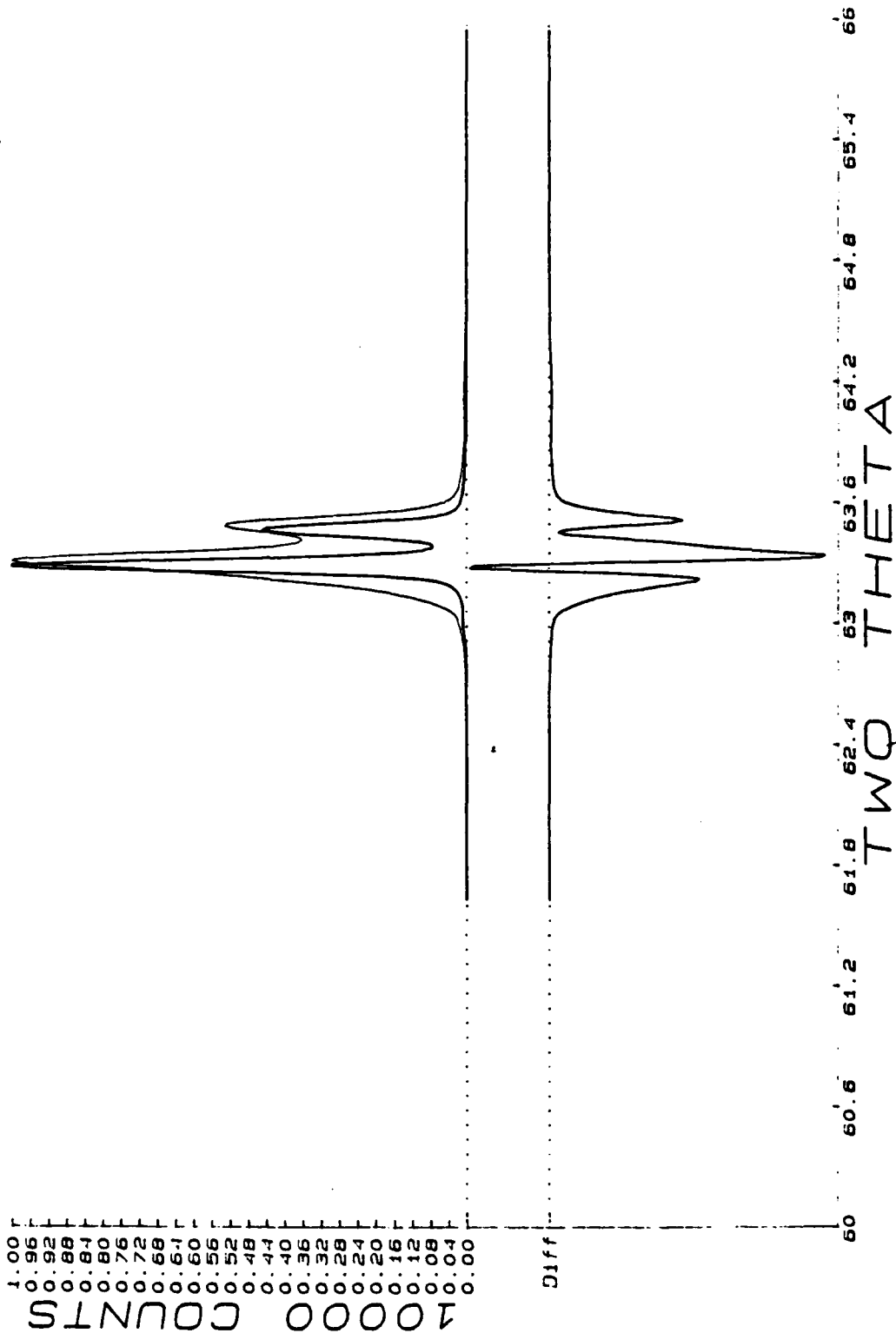


Figure 20. Superposition of substrate curve and substrate plus quaternary layer G0628 with difference shown.

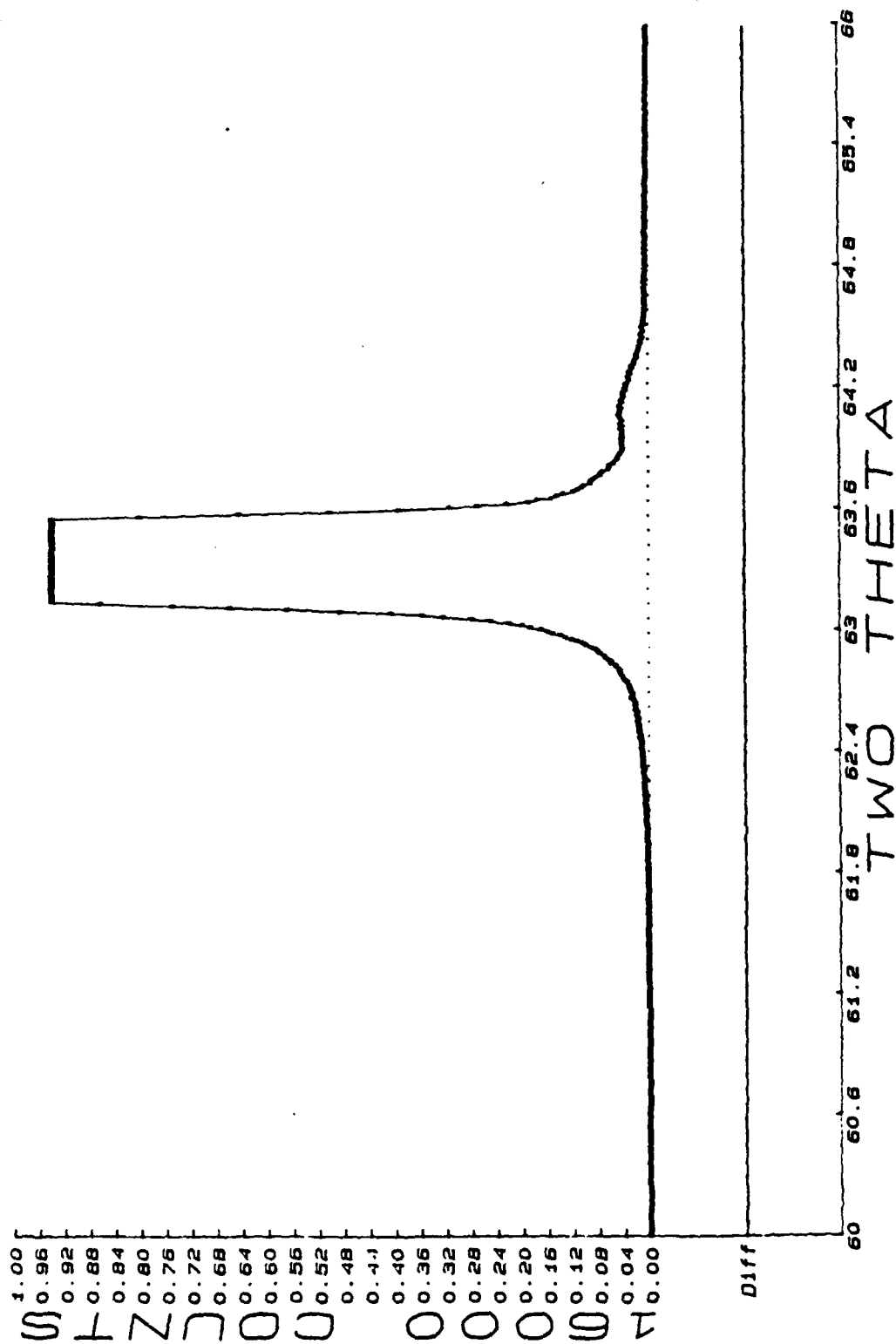
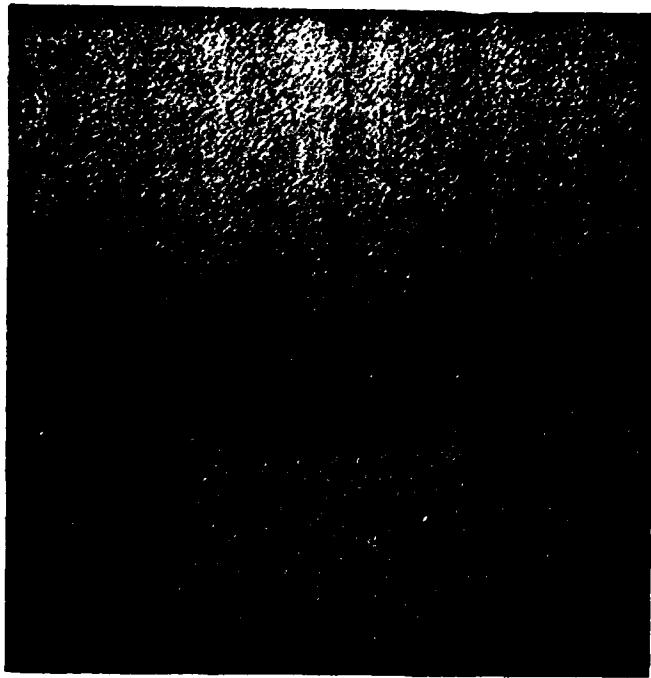
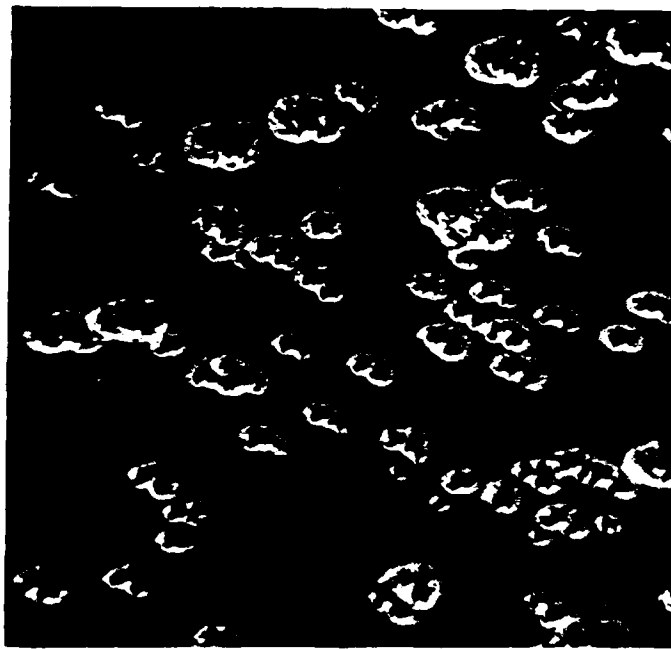


Figure 21. InP substrate with quaternary layer G0628.



G0524



G0628

Figure 22. SEM micrographs of quaternary surfaces. (2000X)

X-ray evaluation of samples G0524 and G0628 also confirm the quality of the layers as described above. Figure 18 shows the diffraction peaks at scattering angles of approximately 30, 63 and 104 degrees for the substrate material. Clear doublets are resolved at each angle corresponding to the copper  $K\alpha_1$  and  $K\alpha_2$  wavelengths. For sample G0524 shown in figure 19, the substrate peaks are clearly seen along with a small broad peak at about  $66^\circ$  that is due to the quaternary layer. The position of the peak corresponds to a lattice constant of 5.68A and the broad shape is due to the poor crystal quality of the layer caused by the large lattice mismatch. Figure 20 compares samples G0628 with the substrate as a standard and shows a plot of the difference. The doublet peak is clearly not resolved as well when the quaternary layer is present, but the peak due to the layer is not seen until the sensitivity is increased as shown in figure 21. The peak shown in figure 21 corresponds to a lattice constant of 5.80A for a mismatch of about 1.0%.

The surface of samples G0522 and G0524 are clear and specular to the naked eye and far better in appearance than the other samples. However, as has been shown, these early samples had the poorest crystal quality. SEM photographs at 2000X of the sample surfaces are shown in Figure 22. From the pictures, it is apparent that even though sample G0524 may appear shiny and smooth to the naked eye, the surface is microscopically very rough. Sample G0628 appears very hazy to the naked eye. The SEM picture shows a pitted surface but the areas between the pits are

much smoother than the surface of G0504. When the lattice mismatch is too great the layer grows in an ordered way but with a unit cell that adjusts slightly to accommodate the strain. This gives the large spots in the RHEED pattern and the broad peak in a x-ray data. At closer lattice match the layer grows single crystal but with dislocations to relieve the strain that grows into pits in the surface.

#### 4.0 CONCLUSIONS

A phosphorus source suitable for InP or quaternary MBE growth was developed and tested. The source cracks the  $P_4$  molecules sufficiently to greatly improve the phosphorus sticking coefficient; the flux can be monitored at all times during growth but the long term stability of the source as presently manufactured is not sufficient for quaternary alloy ratio control; and the source has a useful lifetime compatible with the requirements of good MBE layer growth. A duplicate arsenic source was also developed and tested.

Indium phosphide layers have been grown with excellent room temperature mobility and the necessity of a cracking phosphorus source confirmed. Electrical and optical characterization of the layers indicate that the layers are highly compensated which is consistent with the poor quality of the background vacuum during growth. Little improvement can be anticipated in the present MBE system.

Many quaternary layers have been grown with the new phosphorus and arsenic sources. The best layers grown on InP were matched to within 1.0%. It is expected that with the data obtained thus far, the lattice match can be consistently improved only with a positive, stable real time flux control on both the As and the P sources.

A new MBE system for phosphorus compounds has been designed and is being fabricated. The new system can accommodate 1.5" diameter substrates, has sample rotation, and two stages of

vacuum interlocking for sample introduction. Improved cryoshielding and cryopumping in the growth chamber should result in much improved layers.

## 5.0 REFERENCES

1. Farrow R.F.C., J. Phys. D: Appl. Phys. 7, 1121-124 (1974).
2. Farrow R.F.C., J. Phys. D: Appl: Phys. 7, 2436 (1974).
3. McFee J. H., Miller B.I., & Backmann R. J.J., Electrochem. Soc. 124, 259-272 (1977).
4. Norris M. T. and Stanley C. R., Appl. Phys. Lett 35, 618-620 (1979).
5. Norris M. T., Appl. Phys. Lett 36, 282-282 (1980).
6. Roberts J. S. and Dawson P., Appl. Phys. Lett. 38, 905-957 (1981).
7. Sullivan P. W., Farrow R. F. C., Jones G. R., and Stanley C. R., Gallium Arsenide and Related Compounds, 1980, p. 45-54.
8. Chow R., & Chai Y. G., Appl. Phys. Lett 42 383-385 (1983).
9. Asahi H., Kawamura Y., Ikeda M., & Okamoto H. J., Appl. Phys. 52, 2852 (1981).
10. Tsang W. T., Miller R. C., Capasso F., and Bonner W. A. Appl. Phy. Lett. 41, 467-469 (1982).
11. Meeks E. L., and Eisele F. L., Growth of InP by MBE, Final Report, (1980) ARO contract DAAG 29-80-K-0100.
12. Rode D. L., Phys. Rev B3, 3287 (1971).
13. M. T. Norris and C. R. Stanely, Appl. Phys. lett 35 617 15 Oct. 1979.
14. M. Glisksman and K. Weiser, J. Electrochem. Soc. 105 728 1958.

**END**

**FILMED**

**10-85**

**DTIC**